Abstract

Keywords:

1. Introduction

The search for alternate energy sources which could be categorised under the "green" label has become important area of research in the modern word. Solar, wind power and wave power are some of the examples of these sources. Recently,a new branch of research has been developing to extract energy from flow induced vibrations(Bernitsas et al. (2008)). It has been hypothesized that this technique may work efficiently in areas where regular turbines cannot.

A simple structure that is susceptible to flow-induced vibrations that are suitable for energy extraction are slender structures,such as cylinders, elastically mounted perpendicular to a fluid stream. With regards to a slender body two common types of flow induced vibrations are Vortex Induced Vibrations (VIV) and aeroelastic galloping. Significant research has been carried out by Bernitsas and his team on extracting useful energy from VIV. Some of their significant work includes investigating the influence of physical parameters such as mass ratio (the ratio of the mass of the cylinder and the displaced fluid), Reynolds number, mechanical properties(Raghavan and Bernitsas (2011) ,Lee and Bernitsas (2011)) and location (effect of the bottom boundary) (Raghavan et al. (2009)). However,the possibility of extracting energy using aeroelastic galloping has not been thoroughly investigated. Some theoretical work was carried out by (Barrero-Gil et al. (2010)). Utilizing galloping may be a more viable method to harness energy from flow induced vibrations as it is not bounded by a "lock-in" range of reduced velocities(ratio between the freestream velocity and the product of the natural frequency of the system and the characteristic length).Therefore it is preferable to investigate further the possibility of harnessing energy from flow induced vibrations using aeroelastic galloping.

Real life energy harvesting systems use high damping ratios where the energy generator (e.g electrical generator) puts a significant amount of damping into the system. Therefore it is crucial to investigate the behaviour of aeroleastic galloping scenarios at high damping ratios in order to optimise the system to obtain a acceptable power output.Hence the focus of this paper is concentrated on investigating the mechanical power output of high-damped galloping systems in laminar flow.

According to Païdoussis et al. (2010),Glauert (1919) has provided a criterion for galloping by considering the auto-rotation of an aerofoil. Den Hartog (1956) has provided a theoretical explanation for galloping for iced electric transmission lines. A non-linear

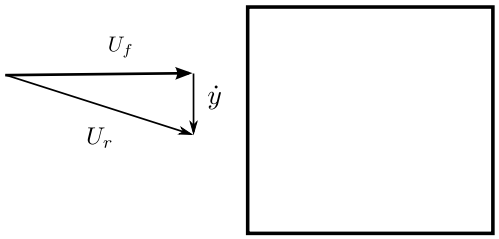

Figure 1:

theoretical aeroelastic model to predict the response of galloping was developed by Parkinson and Smith (1964) based on the quasi-steady state (QSS) theory. Experimental lift and drag data on a fixed square prism at different angles of attack were used as an input for the theoretical model. It essentially used a curve fit of the transverse force to predict the galloping response. The study managed to achieve a good agreement with experimental (wind tunnel) data.Joly et al. (2012) have observed that finite element simulations shows a sudden change in amplitudes below a critical values of the mass ratio, which the (QSS) model fails to reproduce.The Parkinson's equation was essentially modified to account for the vortex shedding and managed to produce the effects to the amplitude at low mass ratios. Barrero-Gil et al. (2010) have investigated the possibility of extracting power from vibrations caused by galloping using quasi-steady state theory. In the conclusions of that paper it was pointed out that in order to obtain a high power to area ratio the mass-damping ($m^*\zeta$) parameter should be kept low as well as the frequency of oscillations should be carefully matched have a good agreement with the size of the cross section. Another interesting conclusion was that energy conversion systems which uses galloping could operate over a large range of flow velocities unlike VIV energy harvesting systems where the factor of energy conversion has a strong dependence on the incoming flow velocity.

2. Come up with title

2.1. Mathematical model (Quasi-steady)

One of the widely used mathematical model to predict the system response under galloping is the Quasi-steady state (QSS) model,incorporated by Parkinson and Smith (1964) for a square cross section. The equation of motion if the body under galloping is given by Eq. (1).The forcing term F_y is given by Eq.(2).

$$(m + m_a)\ddot{y} + c\dot{y} + ky = F_y \tag{1}$$

$$F_y = \frac{1}{2}\rho U^2 C_y \tag{2}$$

The c, k and m_a terms represents the spring stiffness, damping coefficient and the added mas respectively. In the QSS model C_y is determined by an interpolating polynomial based on the stationary lift and drag data. The order of the interpolation polynomial has varied

from study to study (e.g..7^{th} order was used in Parkinson and Smith (1964) and 3^{rd} order polynomial was used in (reference). Ng et al. (2005) concluded that using a 7^{th} order polynomial is sufficient and a polynomial higher than that of 7^{th} order polynomial neither results in a result significantly better result nor does it exhibit an additional amplitudes of oscillation.Thus A 7^{th} order interpolating polynomial is incorporated in this present study.

$$C_y(\alpha) = a_1\left(\frac{\dot{y}}{U}\right) + a_3\left(\frac{\dot{y}}{U}\right)^3 + a_5\left(\frac{\dot{y}}{U}\right)^5 + a_7\left(\frac{\dot{y}}{U}\right)^7 \tag{3}$$

Joly et al. (2012) used a sinusoidal forcing function to the RHS of the oscillator model (Eq. (1)) in order to represent forcing due to VIV. This method provided satisfactory results with the numerical simulations obtained at low mass ratios. This study, the forcing due to VIV is incorporated using a sinusoidal forcing function $F_0 \sin \omega_s t$ added to the RHS. ω_s and F_0 represents shedding frequency and the maximum force due to shedding respectively. Thus, the final equation is represented by Eq. (4).

$$(m+m_a)\ddot{y}+c+\dot{y}+ky=\frac{1}{2}\rho U^2 \mathrm{A}\left(a_1\left(\frac{\dot{y}}{U}\right)+a_3\left(\frac{\dot{y}}{U}\right)^3+a_5\left(\frac{\dot{y}}{U}\right)^5+a_7\left(\frac{\dot{y}}{U}\right)^7\right)+F_0\sin(\omega_s t) \tag{4}$$

This equation could be solved by time integration methods. In this study "Ode 45" routine in MATLAB was used to obtain the solutions.

2.2. Calculation of average power

The dissipated power due to the damper could be expressed as the harvested power output assuming that the other power dissipation due to internal damping such as friction of the system is negligible. Therefore the mean power output could be given by Eq. (5).

$$P_{mean} = \frac{1}{T}\int_0^T (c\dot{y})\dot{y}dt \tag{5}$$

2.3. Parameters used

The stationary data and the FSI data were obtained using a higher order spectral element code which simulates 2D laminar flow.The Reynolds number was kept at 165 as it was pointed out by Sheard et al. (2009) and Tong et al. (2008) that the 3 dimensional transition for a square cylinder occurs at approximately Re-160. F_0 was kept at 0.4937 which was obtained by using a simple linear interpolation on the data of Joly et al. (2012). ω_s was set to 0.98 winch was obtained by a power spectral analysis of the stationary data at 0_0. Stationary C_y data were obtained at different angles of attack ranging from 0^0 to 16^0.The average power was obtained by using Eq. (5) with data sets consisting substantial amount of peaks.In order to obtain a comparison with high Reynolds number power data was obtained using Parkinson and Smith (1964) C_y data.

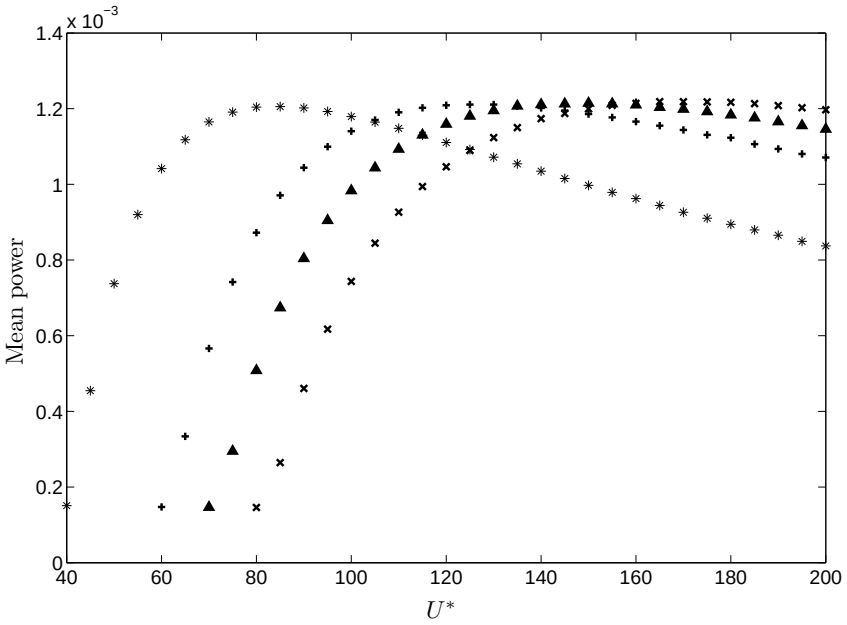

Figure 2: Mean power vs. reduced velocity at different damping ratios at $m^* = 20$. ✳ $\zeta = 0.1$, ✚ $\zeta = 0.15$, ▲ $\zeta = 0.175$ and ✖ $\zeta = 0.2$, at Re = 165.

3. Mean power (Have to use a better title than this)

Mass ratio (m^*) and damping ratio(ζ) was treated as two different variables in the presentation of data. Fig. 2 and 3 shows the mean power against U^* at different ζ and m^*. The data in Fig 2 seems to agree qualitatively with Barrero-Gil et al. (2010) where the peak power was shifting when the damping ratio increased. An interesting observation is that the peak power remains to be constant regardless of the damping ratio where Barrero-Gil et al. (2010) also observed and concluded that the maximum efficiency attainable does not depend the $m^*\zeta$ parameter. A similar observation was made when m^* was increased (Fig.3). However, the peak power at $m^* = 20$ was lesser than the other mass ratios ($m^* = 30, 40, 60$) which produced the same peak mean power. This may be due to the effect of shedding. Joly et al. (2012) an influence of vortex shedding on galloping amplitude at low mass ratios. The data obtained using Parkinson and Smith (1964) C_y curve shows a similar pattern (Fig.6) where a common maximum power could be observed. Hysteresis could be observed in the power curves.

Another interesting observation was that the data at different damping ratios could be collapsed when the mean power was plotted against the damping constant(refer Fig.**??**. This phenomenon could be observed when the mass ratio was changed keeping the damping ratio constant(refer Fig.5). This could be observed at high Reynolds numbers (Using input data of Parkinson and Smith).

The input of the governing equation for galloping (4) does not have a frequency selection (As the shedding term could be disregarded at high mass ratios). Collapsing power data in

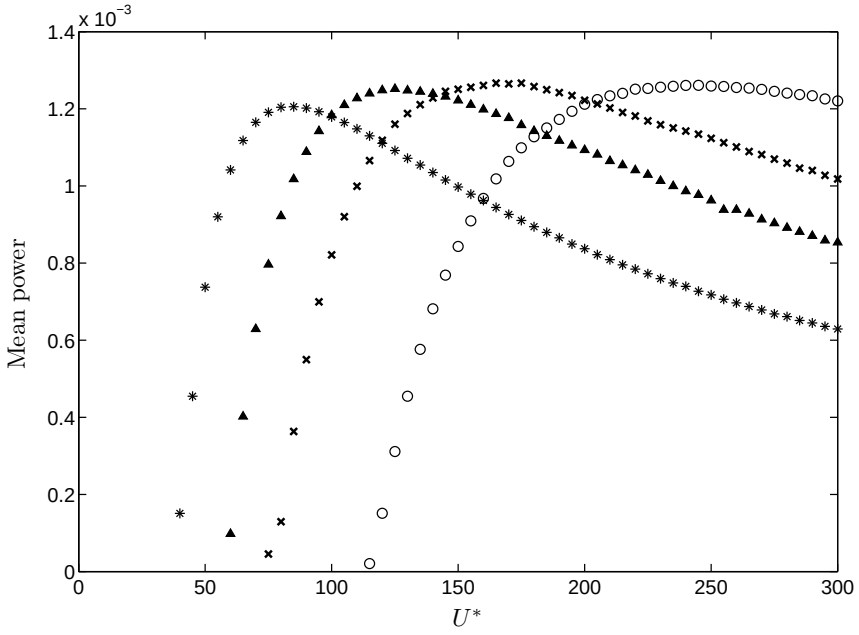

Figure 3: Mean power vs. U^* at different m^* $\zeta = 0.1$ ($\ast$ $m^* = 20$, $\blacktriangle$ $m^* = 30$, $\times$ $m^* = 40$ and $\circ$ $m^* = 60$,, at Re = 165)

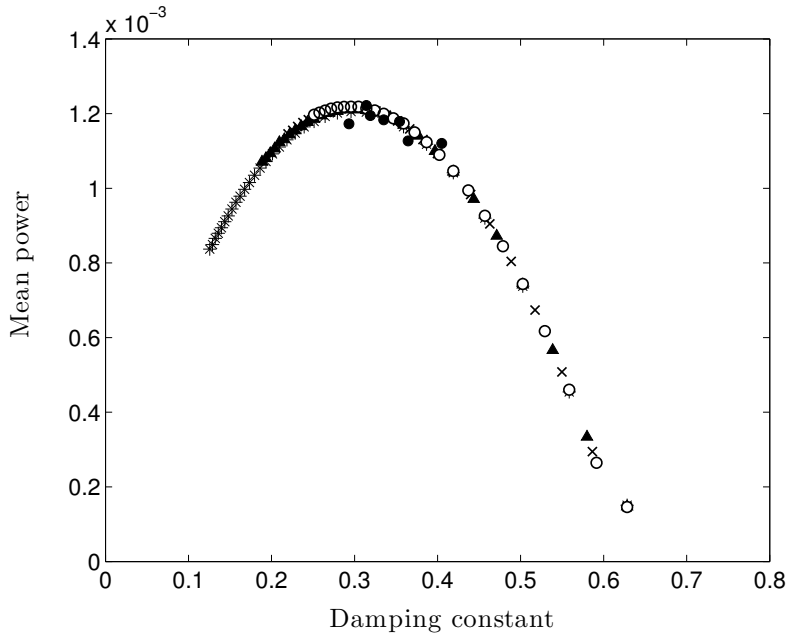

Figure 4: Mean power vs. damping constant at $m^* = 20$. $\ast$ $\zeta = 0.1$, $\blacktriangle$ $\zeta = 0.15$, $\times$ $\zeta = 0.175$ and $\circ$ $\zeta = 0.2$ and $\bullet$ FSI data at Re = 165

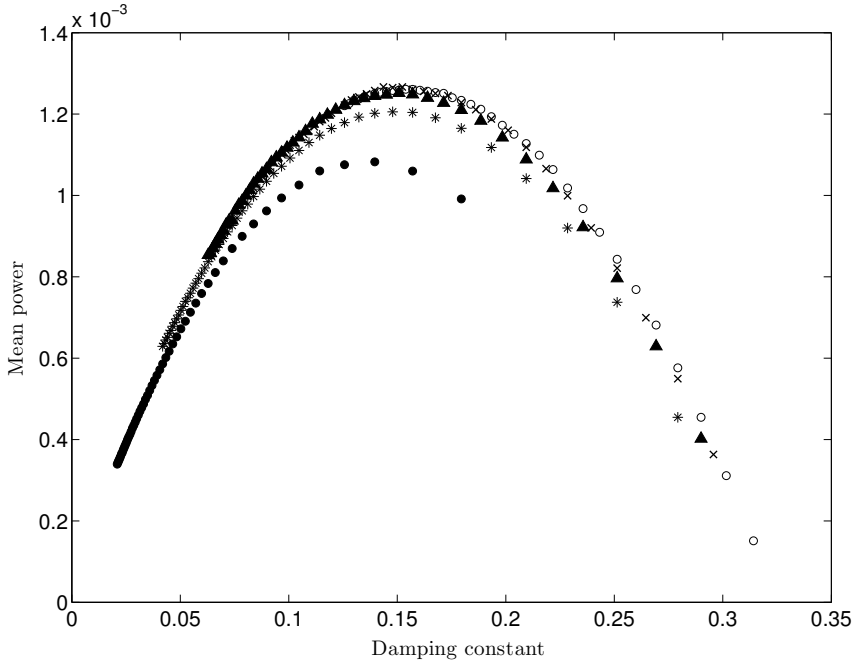

Figure 5: Mean power vs. damping ratio at different m^* $\zeta = 0.1$ (,● $m^* = 10$,✳ $m^* = 20$, ▲ $m^* = 30$, × $m^* = 40$ and ◯ $m^* = 60$, at Re = 165)

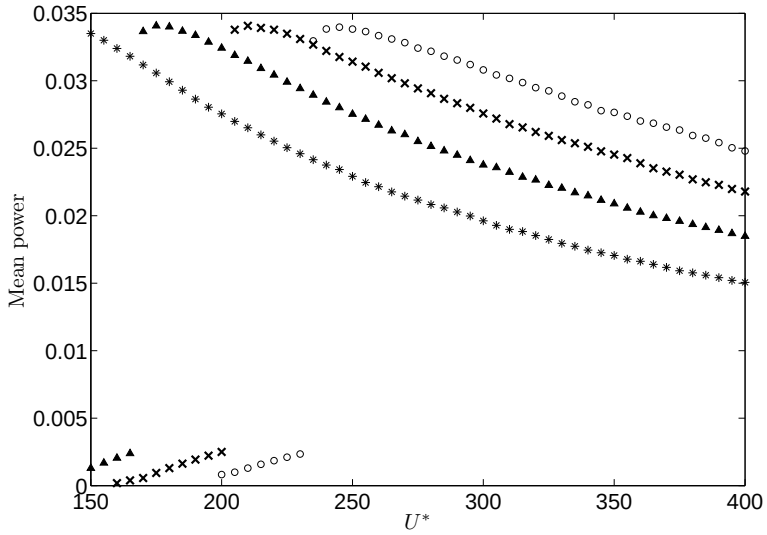

Figure 6:

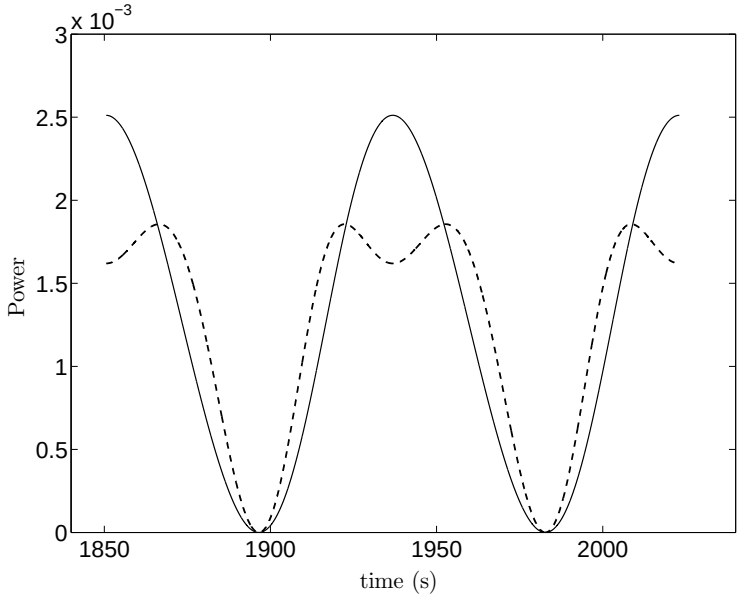

Figure 7:

terms of U^* and ζ implies that there is a frequency selection where ζ and U^* are normalized using the natural frequency.

From an energy point of view, the transfer of power could be expressed from the following equation (where the minor losses are disregarded).

$$P_{fluid\,to\,body} = P_{body\,to\,fluid} + P_{external\,damper} \tag{6}$$

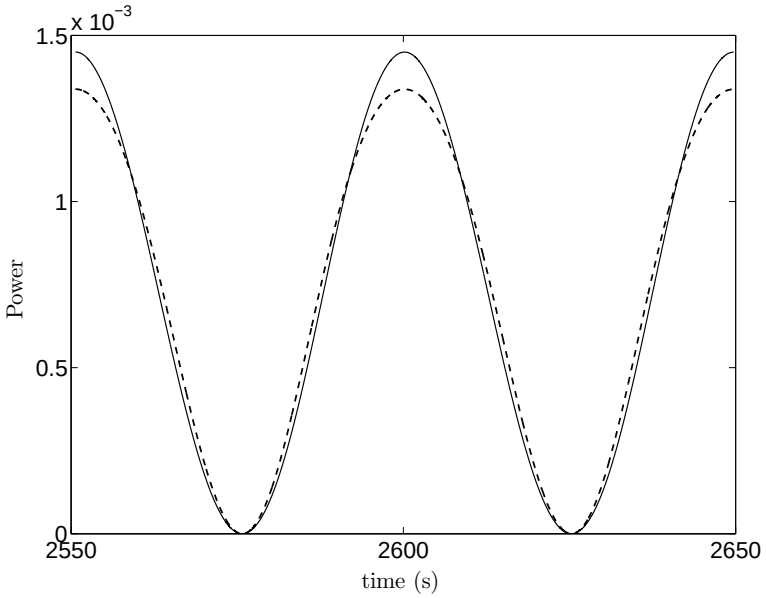

Figure 8:

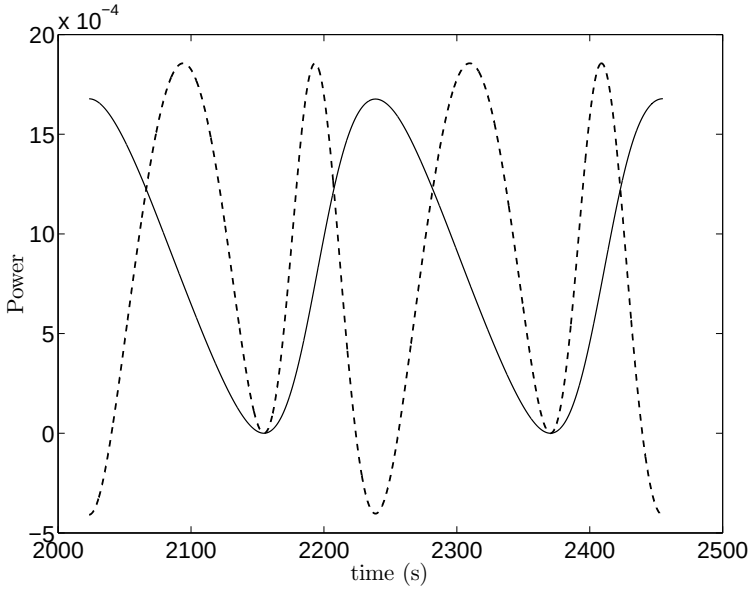

Figure 9:

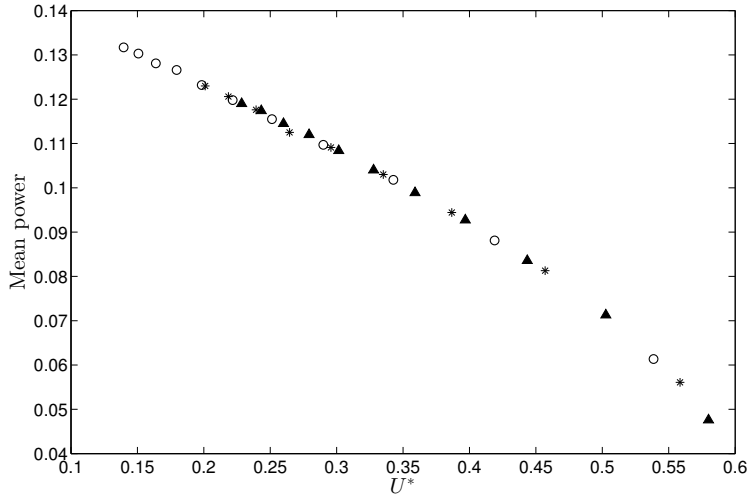

Figure 10: Velocity amplitude vs. damping constant at $m^* = 20$. $\circ$ $\zeta = 0.075$, $\ast$ $\zeta = 0.1$, $\blacktriangle$ and $\zeta = 0.15$, at Re = 165

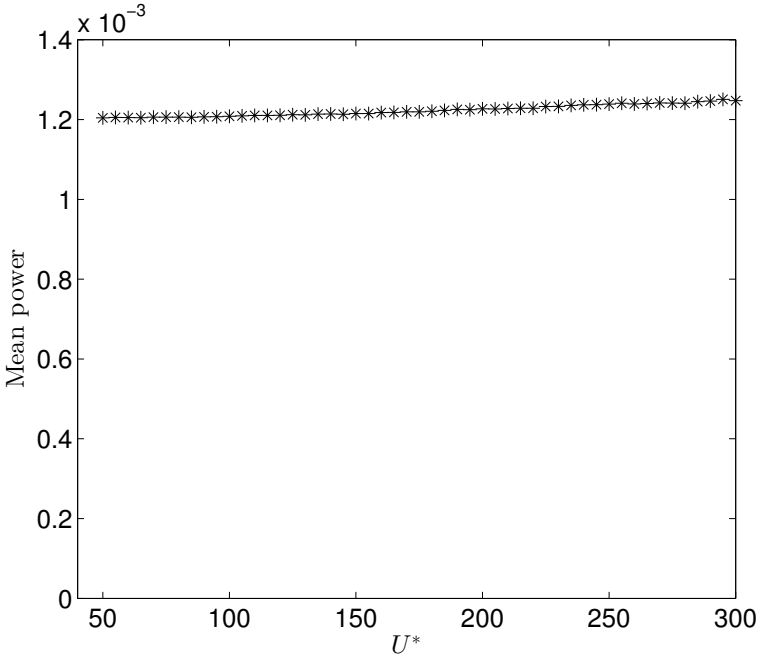

Figure 11: Plot of mean power at damping factor = 2.99

References

Barrero-Gil, A., Alonso, G., Sanz-Andres, A., Jul. 2010. Energy harvesting from transverse galloping. Journal of Sound and Vibration 329 (14), 2873–2883.

Bernitsas, M. M., Raghavan, K., Ben-Simon, Y., Garcia, E. M. H., 2008. VIVACE (Vortex Induced Vibration Aquatic Clean Energy): A new concept in generation of clean and renewable energy from fluid flow. Journal of Offshore Mechanics and Arctic Engineering 130 (4), 041101–15.

Den Hartog, J. P., 1956. Mechanical Vibrations. Dover Books on Engineering. Dover Publications.

Glauert, H., 1919. The rotation of an aerofoil about a fixed axis. Tech. rep., Advisory Committee on Aeronautics R and M 595. HMSO, London.

Joly, A., Etienne, S., Pelletier, D., Jan. 2012. Galloping of square cylinders in cross-flow at low Reynolds numbers. Journal of Fluids and Structures 28, 232–243.

Lee, J., Bernitsas, M., Nov. 2011. High-damping, high-Reynolds VIV tests for energy harnessing using the VIVACE converter. Ocean Engineering 38 (16), 1697–1712.

Ng, Y., Luo, S., Chew, Y., Jan. 2005. On using high-order polynomial curve fits in the quasi-steady theory for square-cylinder galloping. Journal of Fluids and Structures 20 (1), 141–146.
URL http://linkinghub.elsevier.com/retrieve/pii/S0889974604001215

Païdoussis, M., Price, S., de Langre, E., 2010. Fluid-Structure Interactions : Cross-Flow-Induced Instabilities. Cambridge University Press.

Parkinson, G. V., Smith, J. D., 1964. The square prism as an aeroelastic non-linear oscillator. The Quarterly Journal of Mechanics and Applied Mathematics 17 (2), 225–239.

Raghavan, K., Bernitsas, M., Apr. 2011. Experimental investigation of Reynolds number effect on vortex induced vibration of rigid circular cylinder on elastic supports. Ocean Engineering 38 (5-6), 719–731.

Raghavan, K., Bernitsas, M. M., Maroulis, D. E., 2009. Effect of Bottom Boundary on VIV for Energy Harnessing at $8 \times 10^3 < Re < 1.5 \times 10^5$. Journal of Offshore Mechanics and Arctic Engineering 131 (3), 031102.

Sheard, G. J., Fitxgerald, M. J., Ryan, K., Jun. 2009. Cylinders with square cross-section: wake instabilities with incidence angle variation. Journal of Fluid Mechanics 630, 43.

Tong, X., Luo, S., Khoo, B., Oct. 2008. Transition phenomena in the wake of an inclined square cylinder. Journal of Fluids and Structures 24 (7), 994–1005.
URL http://linkinghub.elsevier.com/retrieve/pii/S088997460800025X